

¹H NMR Chemical Shift and Intrinsic Acidity of Hydroxyl Groups. Ab Initio Calculations on Catalytically Active Sites and Gas-Phase Molecules

Ulrich Fleischer,[†] Werner Kutzelnigg,[†] Andreas Bleiber,[‡] and Joachim Sauer^{*‡}

Contribution from the Lehrstuhl für Theoretische Chemie, Ruhr Universität Bochum, D-44780 Bochum, Germany, and the Max-Planck-Gesellschaft, Arbeitsgruppe Quantenchemie an der Humboldt-Universität, Rudower Chaussee 5, Geb 2.1, D-12484 Berlin, Germany

Received December 11, 1992. Revised Manuscript Received March 29, 1993

Abstract: For the molecules H_nXOH (X = H, B, C, N, O, F, Al, Si, P, S, Cl); C₂H₅OH, CF₃CH₂OH, and CF₃OH; B(OH)₃, Al(OH)₃, Si(OH)₄, and OP(OH)₃; H₃AlOPH₂OH and H₃POAlH₂OH; HO(H)Al(OH)₃, H₃SiO(H)Al(OH)₃, H₃SiO(H)AlH₃, and H₃SiO(H)BH₃; and (AlH₂OH)₂ and ((HO)₂AlOH)₂, some of which are models of surface hydroxyl groups, ab initio SCF calculations are performed of both the ¹H NMR chemical shifts and the deprotonation energies. As the latter are a measure of acidity the results obtained can be used to check whether the postulated property–reactivity relation between the chemical shift of the hydroxyl proton and its acidity exists. We find that this is not the case for the general set of systems studied. The reason is that the lone pairs on oxygen and the X–O bond make non-constant and non-negligible contributions to the chemical shift. However, for the limited set of surface hydroxyls which are bonded to B, Al, Si, or P completely coordinated by oxygen atoms, such a relation can be justified.

1. Introduction

Surface hydroxyl groups are the active sites of important heterogeneous catalysts such as zeolites and related solids.^{1,2} The “classical” technique for characterizing these sites is infrared spectroscopy. However, since the development of high-resolution magic-angle-spinning (MAS) NMR techniques for solids (see, e.g. ref 3), ¹H NMR spectroscopy is extensively used to identify different types of surface hydroxyl groups.^{3–8} This method could even gain importance if the ¹H NMR chemical shifts could be used to measure the acidity of hydroxyls and, hence, the intrinsic activity of catalytically active surface sites. A direct relation between the ¹H NMR chemical shift and the intrinsic acidity has been suggested for gas-phase molecules⁹ and for surface hydroxyls.^{4–8} Whether such a relation exists or not is of quite general interest since it is also a prominent example of a property–reactivity relation in chemistry.

The acidity of a molecule is defined as the standard Gibbs free energy of its deprotonation, $\Delta G^\circ_{\text{DP}}$,

$$\Delta G^\circ_{\text{DP}}(T) = \Delta H^\circ_{\text{DP}}(T) - T\Delta S^\circ_{\text{DP}}(T) \quad (1)$$

$\Delta S^\circ_{\text{DP}}$ is the entropy of deprotonation. The standard enthalpy

of deprotonation, $\Delta H^\circ_{\text{HP}}$, is also a suitable acidity measure. Its negative value is defined as the *proton affinity* of the corresponding anion. Relative acidities of gas-phase molecules are derived from measured equilibrium constants of proton transfer reactions.¹⁰ They can be converted into relative *heats of deprotonation* if estimates are available for $\Delta S^\circ_{\text{DP}}$ from statistical mechanics.¹⁰ Absolute $\Delta G^\circ_{\text{DP}}$ and $\Delta H^\circ_{\text{DP}}$ scales are established with use of a few absolute values known from thermodynamic cycles.¹⁰ For the intrinsic acidity of surface hydroxyls the same definition can be used provided that entropy effects that arise from distribution and concentration of sites on the surface are neglected. Thus, it is possible to put surface sites and gas-phase molecules onto one and the same acidity scale.

Acidity and heat of deprotonation as thermodynamic functions defined for a reaction depend both on the neutral reactant molecule and the anion formed, while the chemical shift is a property of the unperturbed reactant molecule alone. A possible relation between these two quantities relies on the following arguments.^{5,6} (1) Deprotonation is easier the higher the net charge on the hydrogen atom in the molecule is. (2) The higher the net charge on the hydrogen atom is (i.e. the lower the electron density), the less the nucleus is shielded. As neither of these arguments can be rigorously derived from molecular orbital theory (see, e.g., refs 11 and 12), the suggested relation can only emerge from empirical evidence. For molecules in the gas phase, measurements of both the relative proton affinities and ¹H NMR chemical shifts are available. An example is the study of Chauvel and True on alcohols.⁹ For surface hydroxyls, an attempt has been made to deduce relative proton affinities from the OH frequency shifts observed on formation of their complexes with proton acceptor molecules.¹³ The results have been plotted against observed ¹H NMR chemical shifts,¹⁴ but the correlation found is not convincing. Among the 18 hydroxyl groups considered, there are 7

(10) Bartmess, J. E.; Scott, J. A.; McIver, R. T., Jr. *J. Am. Chem. Soc.* **1979**, *101*, 6046.

(11) Kawakami, H.; Yoshida, S.; Yonezawa, T. *J. Chem. Soc., Faraday Trans.* **1984**, *80*, 205.

(12) Pople, J. A.; Schneider, W. G.; Bernstein, H. J. *High-Resolution Nuclear Magnetic Resonance*; McGraw-Hill: New York, 1959; p 175.

(13) Paukshtis, E. A.; Yurtchenko, E. N. *Usp. Khim.* **1983**, *52*, 426.

(14) Mastikhin, V. M.; Mudrakovsky, I. L.; Nosov, A. V. *Bruker Report* **1989**, *2*, 18.

[†] Ruhr Universität Bochum.

[‡] Max-Planck-Gesellschaft.

(1) Jacobs, P. A. *Carbionogenic Activity of Zeolites*; Elsevier: Amsterdam, 1977.

(2) Maxwell, I. E.; Stork, W. H. J. In *Introduction to Zeolite Science and Practice*. Vol. 85. *Studies in Surface Science and Catalysis*; van Bekkum, H., Flanigen, E. M., Jansen, J. C., Eds.; Elsevier: Amsterdam, 1991.

(3) Engelhardt, G.; Michel, D. *High-Resolution Solid-State NMR of Silicates and Zeolites*; Wiley: Chichester, 1987.

(4) Pfeifer, H.; Freude, D.; Hunger, M. *Zeolites* **1985**, *5*, 274.

(5) Freude, D.; Hunger, M.; Pfeifer, H. *Z. Phys. Chem. (Frankfurt/Main)* **1987**, *152*, 171.

(6) Hunger, M.; Pfeifer, H. In *Innovation in Zeolite Materials Science*. Vol. 37. *Studies in Surface Science and Catalysis*; Grobet, P. J., Mortier, W. J., Vasant, E. F., Schulz-Ekloff, G., Eds.; Elsevier: Amsterdam, 1987; p 155.

(7) Brunner, E.; Freude, D.; Hunger, M.; Pfeifer, H.; Staudte, B. In *Zeolite Chemistry and Catalysis*. Vol. 69. *Studies in Surface Science and Catalysis*; Jacobs, P. A., Jaeger, N. I., Kubelkova, L., Wichterlova, B., Eds.; Elsevier: Amsterdam, 1991; p 453.

(8) Pfeifer, H.; Freude, D.; Kärger, J. In *Catalysis and Adsorption by Zeolites*. Vol. 65. *Studies in Surface Science and Catalysis*; Ohlmann, G., Pfeifer, H., Fricke, R., Eds.; Elsevier: Amsterdam, 1991; p 89.

(9) Chauvel, J. P., Jr.; True, N. S. *Chem. Phys.* **1985**, *95*, 435.

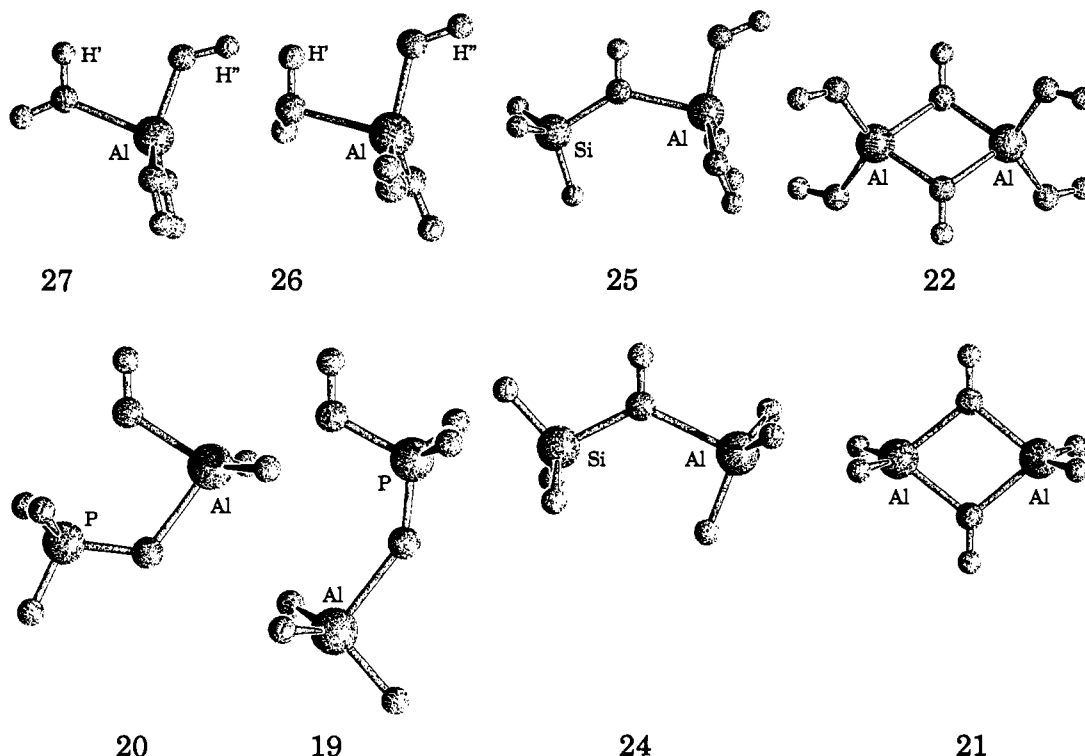


Figure 1. Some models studied (from left to right): upper row—HO(H)Al(OH)₃/C_s and C₁, H₃SiO(H)Al(OH)₃, and ((HO)₂AlOH)₂; lower row—H₃POAlH₂OH, H₃AlOPH₂OH, H₃SiO(H)AlH₃, and (AlH₂OH)₂. The numbers refer to Table I.

within a shift range of about 0.5 ppm, but their estimated heat of deprotonation varies widely over almost 500 kJ/mol. Direct measurements of proton affinities of surface hydroxyl groups have not been possible so far.

In this situation quantum chemical *ab initio* calculations provide a unique opportunity to investigate the ¹H NMR chemical shift–acidity relation. The computational approach has the additional advantage that the assumptions of a chemical shift–acidity relation can be individually checked and that different contributions to both the acidity and the chemical shift can be analyzed. The acidity can be approximated by the energy of deprotonation, Δ*E*_{DP}, which differs from Δ*H*^o_{DP} by nuclear motion corrections only:

$$\Delta H^{\circ}_{\text{DP}}(T) = \Delta E_{\text{DP}} + \Delta E^{\text{zp}}_{\text{DP}} + \Delta H^{\circ}_{\text{therm}}(T) \quad (2)$$

The thermal corrections, Δ*H*_{therm}(*T*), are tiny, about 5 kJ/mol (see, e.g. ref 15), and do not contribute to relative acidities. The zero-point vibrational energy changes, Δ*E*^{zp}_{DP}, are somewhat larger, between 30 and 40 kJ/mol (*vide infra*), but vary little for different hydroxyls and do not affect relative heats of deprotonation beyond an uncertainty of ±5 kJ/mol.

Quantum chemical calculations have been performed of the energy of deprotonation (as a measure of acidity) and of the ¹H NMR shielding constants for a variety of hydroxyls in molecules and on surfaces. For the latter, models were designed that put the hydroxyls in the same coordination environment that they have on the catalyst surface. It turns out that the correlation found by Chauvel and True⁹ rests on the fact that all hydroxyls considered are C–OH groups. Considering all XOH groups studied no correlation can be found. We will arrive at the conclusion that a correlation can only be assumed for limited sets of hydroxyl groups in sufficiently similar bonding environments. Calculation of the charges on the acidic proton and of the contributions of different electron pairs to the chemical shift shows that the deviations from a correlation are mainly due to the fact

that the lone pairs on oxygen and the OX bond make non-constant and non-negligible contributions to the proton chemical shift.

2. Systems Studied

The systematic series H_{*n*}XOH, with X/*n* = H/0, B/2, C/3, N/2, O/1, F/0, Al/2, Si/3, P/2, S/1, and Cl/0, has been augmented by the substitution products C₂H₅OH, CF₃OH, and CF₃CH₂OH; by Al(OH)₃, Si(OH)₄, and OP(OH)₃; and by the protonated species H₃O⁺, CH₃OH₂⁺, and P(OH)₄⁺.

H₂BOH, H₂AlOH, and H₃SiOH are the most primitive, and B(OH)₃, Al(OH)₃, and Si(OH)₄ are improved models of free B–OH, Al–OH, and Si–OH surface hydroxyl groups. OP(OH)₃ is our model for P–OH groups on catalysts modified by phosphoric acid.

H₃AlOPH₂OH and H₃POAlH₂OH (Figure 1) are models for terminal surface hydroxyl groups on aluminum phosphates (AlPO's) and, in first approximation, may also represent such groups on surfaces of silicon-substituted aluminum phosphate catalysts (SAPO's).

For bridging SiO(H)Al, SiO(H)B, and AlO(H)Al hydroxyl groups the HO(H)Al(OH)₃, H₃SiO(H)Al(OH)₃, H₃SiO(H)AlH₃, H₃SiO(H)BH₃, (AlH₂OH)₂, and ((HO)₂AlOH)₂ models (Figure 1) have been adopted. The terminal OH groups of these molecules can serve as additional models of free Al–OH and Si–OH groups.

The data points of the different groups of systems are represented by different symbols in Figures 2–5.

3. Calculations

Theoretical geometries^{16,17} and harmonic vibrational frequencies are obtained by SCF calculations employing the 6-31G* basis set.¹⁸ To compensate for a known systematic overestimation of frequencies calculated that way, a uniform scaling factor of

(15) Sauer, J.; Ahlrichs, R. *J. Chem. Phys.* **1990**, *93*, 2575.

(16) Sauer, J. *J. Phys. Chem.* **1987**, *91*, 2315.

(17) Sauer, J.; Bleiber, A.; Hill, J.-R.; Ahlrichs, R., paper in preparation.

Table I. ¹H NMR Shielding Constants and Anisotropies (σ_H and $\Delta\sigma_H^a$ in ppm), Contribution of Individual Localized Molecular Orbitals (LMO) to the Shielding Constants, and Deprotonation Energies (ΔE_{DP} in kJ/mol)

molecule/point group	σ_H	$\Delta\sigma_H^a$	LMO contributions			ΔE_{DP}
			OH ^b	lp ^c	OX ^d	
1 H ₂ O/C _{2v}	30.9	21.4	17.2	4.8	4.0	1700
2 BH ₂ OH/C _s	26.5	13.1	17.2	3.5 ^e	3.5 ^e	1523
3 CH ₃ OH/C _s	31.9	21.6	17.7	5.4	3.5	1677
4 C ₂ H ₅ OH/C _s	31.4	22.5	17.7	5.2	3.5	1671
5 CF ₃ CH ₂ OH/C ₁	30.5	21.0	17.1	5.1	3.4	1591
6 CF ₃ OH/C _s	28.3	19.7	16.4	4.4	3.5	1460
7 NH ₂ OH/C _s	28.9	19.5	17.6	4.4	2.9	1701
8 H ₂ O ₂ /C ₂	26.9	15.1	18.0	3.1	2.2	1625
9 FOH/C _s	21.9	12.5	18.4	0.6	1.5	1561
10 AlH ₂ OH/C _s	29.7	20.0	16.5	4.5 ^e	4.5 ^e	1615
11 SiH ₃ OH/C _s	31.0	22.2	16.3	5.3	4.4	1561
12 PH ₂ OH/C _s	30.8	23.0	16.7	5.4	3.6	1569
13 HSOH/C ₁	30.7	24.8	16.6	5.5	3.2	1587
14 ClOH/C _s	30.8	26.5	16.6	5.0	2.7	1539
15 B(OH) ₃ /C _{3h}	29.0	19.5	16.5	4.8	3.5	1571
16 Al(OH) ₃ /C _{3h}	30.7	24.5	16.2	4.9 ^e	4.9 ^e	1636
17 Si(OH) ₄ /S ₄	29.7	22.8	16.0	5.0	4.3	1563
18 OP(OH) ₃ /C ₃	28.5	20.9	15.8	4.7	4.2	1438 ^f
19 H ₃ AlOPH ₂ OH/C _s	28.7	23.6	15.5	4.9	4.3	1285
20 H ₃ POAlH ₂ OH/C _s	31.2	23.6	16.7	5.2	4.7	1494
21 (AlH ₂ OH) ₂ /D _{2h}	29.3	25.2	15.7	4.8 ^e	4.8 ^e	1448 ^f
22 ((HO) ₂ AlOH) ₂ /S ₂						
AlO(H)Al	28.9	23.2	15.5	4.6 ^e	4.6 ^e	1446 ^f
AlOH	31.0	25.3	16.4	5.1	4.7	
23 H ₃ SiOH·BH ₃ /C _s	29.8	24.2	15.5	5.0	4.4	1403
24 H ₃ SiOH·AlH ₃ /C _s	28.9	23.0	15.2	5.0	4.3	1329
25 H ₃ SiOH·Al(OH) ₃ /C _s						
SiOH	27.8	21.0	14.5	4.8	4.2	1353
AlOH	31.6	25.6	16.6	5.2	4.7	
AlOH (2×)	31.6	23.6	16.7	5.0 ^e	5.0 ^e	
26 H ₂ O·Al(OH) ₃ /C ₁						
HOH'	27.6	20.4	15.3	4.4	3.7	1391 ^f
AlOH''	31.3	25.1	16.6	5.0 ^e	5.0 ^e	
27 H ₂ O·Al(OH) ₃ /C _s						
HOH'	27.2	21.4	15.1	4.3	3.7	1378 ^f
AlOH''	31.6	25.3	16.6	5.1 ^e	5.1 ^e	
28 H ₃ O ⁺ /C _{3v}	23.5	23.3	13.3	3.8	3.2	734
29 CH ₃ OH ₂ ⁺ /C _s	25.7	24.2	14.4	4.4	3.3	804
30 H ₄ PO ₄ ⁺ /S ₄	25.6	23.2	14.1	4.3	3.7	882 ^f

^a $\Delta\sigma_H = \sigma_{33} - 1/2(\sigma_{22} + \sigma_{11})$ with $\sigma_{33} \geq \sigma_{22} \geq \sigma_{11}$. ^b OH bond orbital. ^c Lone pair orbital. ^d OX bond orbital. ^e Average value of the three localized orbitals on O other than the OH bond orbital. ^f 5d set.

0.89 was used¹⁸ when calculating zero-point vibrational energies. Deprotonation energies are evaluated at the difference between the SCF energies of the anion and the parent molecule at their respective equilibrium geometries. Since diffuse functions are known to be essential in describing the electronic structure of anions, in these calculations the 6-31G* basis sets were augmented on the O atom by a set of diffuse sp functions (exponent 0.0845)¹⁹ and on the hydrogen atoms of the hydroxyl groups by a set of p polarization functions (exponent 1.1).¹⁸ This basis set may be denoted 6-31(+)*G*(*) with the parentheses indicating that the additional functions have been added to selected atoms only. The so defined approximation level, 6-31(+)*G*(*)//6-31G*, yields relative deprotonation energies accurate to a few kJ/mol, although there is a systematic deviation of about 30 kJ/mol from accurate deprotonation energies (vide infra, cf. refs 17 and 18). The TURBOMOLE²⁰ and GAUSSIAN 90²¹ codes are employed.

¹H NMR chemical shifts are calculated by the coupled Hartree-Fock method in terms of localized molecular orbitals and individual gauge origins for different MOs (IGLO method) as described in refs 22–24 and reviewed in ref 25. The [7s,6p,2d/5s,4p,1d/3s,1p] basis sets of contracted Gaussian orbitals were

(18) Hehre, W. J.; Radom, L.; Schleyer, P. v. R.; Pople, J. A. *Ab initio Molecular Orbital Theory*; Wiley: New York, 1986.
 (19) Chandrasekar; Schleyer, P. v. R. *J. Am. Chem. Soc.* **1981**, *103*, 5609.

Table II. Observed^{a,b} and Calculated^c Deprotonation Enthalpies ($\Delta H^\circ DP(298)$ in kJ/mol)

	molecule	obsd ^{a,b}	calcd ^c
1	H ₂ O	1635 ^a	1671
3	CH ₃ OH	1595 ± 2 ^a	1642
4	C ₂ H ₅ OH	1582 ± 8 ^a	1637
5	CF ₃ CH ₂ OH	1514 ± 15 ^a	1559
8	H ₂ O ₂	1573 ± 9 ^a	1595
11	SiH ₃ OH	1502 ± 21 ^b	1534
14	ClOH	1502 ± 9 ^a	1513
28	H ₃ O ⁺	697 ^a	708
29	CH ₃ OH ₂ ⁺	761 ^a	778

^a Reference 28. ^b Reference 29. ^c Equation 2, $\Delta H^\circ_{therm} = -5$ kJ/mol.

derived from Huzinaga's (11s,7p/9s,5p/5s) primitive sp sets²⁶ in the contraction (5,1,1,1,1,1,1;2,1,1,1,1,1/5,1,1,1,1;2,1,1,1/3,1,1) and augmented by the following polarization functions (exponents in parentheses): two d sets on Al (1.2 and 0.3), Si and P (1.4 and 0.35), S and Cl (1.6 and 0.4); one d set on B (0.7), C–F (1.0); and one p set on H (0.65). In previous studies on chemical shifts of molecules containing second-row elements^{25,27} the conclusion was reached that such basis sets may serve as a standard since they yield rather acceptable results.

4. Results and Discussion

Table I shows the calculated deprotonation energies and ¹H shielding constants. The use of localized orbitals in the IGLO method allows the shielding constant to be split into contributions from the individual orbitals. Table I shows not only the contribution from the OH bond orbital but also the contributions of the other orbitals localized on the oxygen atom of the OH group, namely the XO bond orbital and the two lone pair orbitals, which may account for up to almost one-half of the shielding constants.

Before the existence of a correlation between deprotonation energies and shielding constants is discussed, it will be checked how well the calculated data agree with the available observed ones.^{28,29} Table II compares deprotonation enthalpies calculated according to eq 2 from deprotonation energies (Table I), calculated zero-point vibrational corrections, and a uniform value of –5 kJ/mol for ΔH_{therm} (e.g. ref 15) with observed deprotonation enthalpies. The resulting systematic deviation of –33 ± 22 kJ/mol is due to the basis set truncation and neglected electron correlation effects. This follows from a comparison of the deprotonation energies of Table I with the results of highly accurate calculations,¹⁵ which yields differences of –30, –33, and –30 kJ/mol for H₂O, CH₃OH, and SiH₃OH. The scatter of ±22 kJ/mol does not significantly exceed the uncertainty of some of the observed data. Since the zero-point vibrational energies of

(20) Häser, M.; Ahlrichs, R. *J. Comput. Chem.* **1989**, *10*, 104. Ahlrichs, R.; Bär, M.; Häser, M.; Horn, H.; Kölmel, C. *Chem. Phys. Lett.* **1989**, *162*, 165. Horn, H.; Weiss, H.; Häser, M.; Ehrig, M.; Ahlrichs, R. *J. Comput. Chem.* **1991**, *12*, 1058.

(21) Frisch, M. J.; Head-Gordon, M.; Trucks, G. W.; Foresman, J. B.; Schlegel, H. B.; Raghavachari, K.; Robb, M.; Binkley, J. S.; Gonzalez, C.; Defrees, D. J.; Fox, D. J.; Whiteside, R. A.; Seeger, R.; Melius, C. F.; Baker, J.; Martin, L. R.; Kahn, L. R.; Stewart, J. J. P.; Topiol, S.; Pople, J. A. *Gaussian 90*; Gaussian Inc.: Pittsburgh, PA, 1990.

(22) Kutzelnigg, W. *Isr. J. Chem.* **1980**, *19*, 193.

(23) Schindler, M.; Kutzelnigg, W. *J. Chem. Phys.* **1982**, *76*, 1919.

(24) Schindler, M.; Kutzelnigg, W. *J. Am. Chem. Soc.* **1983**, *105*, 136C.

(25) Kutzelnigg, W.; Fleischer, U.; Schindler, M. *NMR: Basic Prin. Prog.* **1990**, *23*, 165.

(26) Huzinaga, S. Technical Report, Vols. 1 and 2, University of Alberta, Edmonton, 1971; *J. Chem. Phys.* **1965**, *42*, 1293.

(27) Fleischer, U.; Schindler, M.; Kutzelnigg, W. *J. Chem. Phys.* **1987**, *86*, 6337.

(28) Lias, S. G.; Bartmess, J. E.; Liebman, J. F.; Holmes, J. L.; Levine, R. D.; Mallard, W. G. *J. Phys. Chem. Ref. Data* **1988**, *17*, Suppl. 1.

(29) Damrauer, R.; Simon, R.; Krempp, M. *J. Am. Chem. Soc.* **1991**, *113*, 4431.

Table III. Comparison of Observed and Calculated ^1H NMR Chemical Shifts (δ_{H} (ppm)) for Hydroxyl Protons Relative to Gas-Phase $\text{CH}_3\text{OH}^{\text{a}}$

	obsd		calcd	calcd
CH_3OH	0.0 ^b	CH_3OH	0.0 ^b	
$\text{C}_2\text{H}_5\text{OH}$	0.4 ^c	$\text{C}_2\text{H}_5\text{OH}$	0.5	
H_2O	0.6 ^c	H_2O	1.0	
$\text{CF}_3\text{CH}_2\text{OH}$	1.4 ^c	$\text{CF}_3\text{CH}_2\text{OH}$	1.4	
terminal $\equiv\text{SiOH}$	1.8–2.3 ^d (1.8) ^e	$\text{Si}(\text{OH})_4$	2.2	H_3SiOH 0.9
bridged $\equiv\text{Si}(\text{H})\text{Al}\equiv$	3.8–4.4 ^d (4.0) ^e	$\text{H}_3\text{SiO}(\text{H})\text{Al}(\text{OH})_3$	4.1	$\text{H}_3\text{SiOH}\cdot\text{AlH}_3$ 3.0
free AlOH	(–0.5) to 1.0 ^d (1.0) ^e	$\text{H}_2\text{O}\cdot\text{Al}(\text{OH})_3$	0.2–0.6	
		$\text{H}_3\text{SiO}(\text{H})\text{Al}(\text{OH})_3$	0.3	$(\text{HO})_2\text{AlOPH}_3$ 0.7
		$(\text{HO})_2\text{AlOH}_2$	0.9	
		$\text{Al}(\text{OH})_3$	1.2	
bridged $\text{AlO}(\text{H})\text{Al}$	2.5–3.6 ^d (2.5) ^e	$(\text{HO})_2\text{AlOH}_2$	3.0	$(\text{H}_2\text{AlOH})_2$ 2.6
BOH	2.5 \pm 0.2 ^f	$\text{B}(\text{OH})_3$	2.9	
POH	1.5–4.0 ^f (2.9) ^g	H_3PO_4	3.3–3.6	$\text{H}_3\text{AlOPH}_2\text{OH}$ 3.2

^a The experimental shift of methanol relative to gaseous TMS is 0.02 ppm (ref 9); if the molecule contains different types of hydroxyl groups that one referred to is indicated by an underbar. ^b By definition. ^c Reference 9. ^d Reference 8. ^e Reference 32. ^f Reference 7. ^g Reference 38.

all systems in Table II are between 30 and 40 kJ/mol, *relative* deprotonation energies can be safely used instead of *relative* heats of deprotonation. Also for systems of other structure types, e.g. bridging hydroxyl groups, the calculated zero-point vibrational energies are about 30 kJ/mol: $\text{HO}(\text{H})\text{Al}(\text{OH})_3$, 32 kJ/mol; $\text{H}_3\text{SiO}(\text{H})\text{Al}(\text{OH})_3$, 32 kJ/mol; $\text{H}_3\text{SiO}(\text{H})\text{AlH}_3$, 31 kJ/mol; and $(\text{HO})_2\text{AlOH}_2$, 29 kJ/mol.

Among the systems studied, only for H_2O , CH_3OH , $\text{C}_2\text{H}_5\text{OH}$, and $\text{CF}_3\text{CH}_2\text{OH}$ can the calculated σ_{H} values be compared with results of gas-phase measurements.⁹ This is done in Table III. The shielding in CH_3OH is used as reference and the chemical shift, $\delta(\text{X})$, in molecule X is as usually defined as $\delta(\text{X}) = \sigma(\text{CH}_3\text{OH}) - \sigma(\text{X})$ i.e. $\delta > 0$ means that the proton is less shielded in X than in CH_3OH (downfield shift). The table shows that the IGLO method used in this study in combination with a flexible basis set involving polarization functions also on H yields results which deviate by a few tenths of a ppm from observed values. This fits in to the mean deviation of 0.5 ppm between calculated and observed proton chemical shifts for a broad variety of molecules involving different X–H bonds.²⁵

When a higher accuracy is attempted, attention should be also paid to the molecular geometry for which the calculations are performed. The difference between theoretical equilibrium structures (e.g. 6-31G* results as used in this study) and observed structures may change the σ_{H} values by several tenths of a ppm. This can be concluded from the results for H_2O and CH_4 of refs 23 and 24 and from additional calculations that we have made on CH_3OH and SiH_3OH . For an observed geometry of CH_3OH ,³⁰ the calculation yields $\sigma_{\text{H}} = 32.2$ ppm, while $\sigma_{\text{H}} = 31.9$ ppm results for the 6-31G* geometry (Table I). For SiH_3OH the chemical shift is predicted to vary by $-0.93/+1.00$ ppm and ± 0.19 ppm when the OH bond distance and the SiOH bond angle change by ± 2.5 pm and $\pm 2.5^\circ$, respectively. On this basis a total change of 1.1 ppm is predicted when the 6-31G* equilibrium geometry is replaced by the vibrationally averaged internal coordinates of ref 31. For the purpose of this study, however, it is important that geometries of uniform quality are used for all the molecules considered, as the 6-31G* equilibrium geometry.

Table III also shows the shift ranges of lines observed in the ^1H MAS NMR spectra of zeolitic catalysts and compares them with calculated shifts for models of surface hydroxyls. The latter have been grouped into two sets which differ in the design of the models. In the first set the central B, Al, and Si atoms have a complete oxygen coordination, while in the less realistic second group some hydrogen atoms are bonded directly to these central atoms. The calculated shifts of $\text{Si}(\text{OH})_4$ and $\text{SiH}_3\text{OH}\cdot\text{Al}(\text{OH})_3$ relative to CH_3OH (Table I) fall into the shift range observed

Table IV. Results of Linear Regression Analysis – Correlation Coefficient, r , and Standard Deviations, s (ΔE_{DP} and σ_{H} in kJ/mol and ppm, respectively)

plot	all 30 systems		cations 28–30 excluded		cations and systems 2, 7, 8, 9 excluded	
	r	s	r	s	r	s
$\Delta E_{\text{DP}} - \sigma_{\text{H}}$	0.61	194	0.32	110	0.91	105
$\Delta E_{\text{DP}} - p_{\text{H}}$	0.94	85	0.89	53	0.93	90
$\sigma_{\text{H}} - p_{\text{H}}$	0.53	2.0	0.30	2.0	0.82	1.2
$\sigma_{\text{H}}(\text{OH}) - p_{\text{H}}$	0.89	0.56	0.83	0.55	0.94	0.39

for $\equiv\text{SiOH}$ and $\equiv\text{SiO}(\text{H})\text{Al}\equiv$ surface hydroxyls in zeolites.^{3–8,32,33} For example, a 500-MHz ^1H MAS NMR study on HZSM-5 zeolites yielded a shift difference of 2.2 ± 0.1 ppm between terminal and bridging hydroxyl groups.³² The IGLO calculations for the molecular models of these surface hydroxyls predict a difference of 1.9 ppm (cf. Table III), in close agreement with the observations.

The assignment of shift ranges for other types of surface hydroxyls is less clear. Terminal Al–OH groups are expected to give rise to signals in the range between -0.5 and 1.0 ppm provided they are free of interactions.⁸ The calculations show that the shifts depend on the coordination number of Al and predict values of 0.2 – 0.6 ppm for hydroxyls on 4-fold coordinated aluminum, $^{\text{IV}}\text{Al}\text{--OH}$ (models 22 and 25–27), and of about 1.2 ppm for free hydroxyls on 3-fold coordinated aluminum, $^{\text{III}}\text{Al}\text{--OH}$ (model 16). Moreover, the calculated shift of bridging $^{\text{IV}}\text{Al}\text{--O}(\text{H})\text{--}^{\text{IV}}\text{Al}$ groups (3.0 ppm for model 22) falls into the range which is assigned to hydroxyls connected with extra-framework material in dealuminated zeolites. The calculated shifts of $\text{B}(\text{OH})_3$ and H_3PO_4 are representative of $(\text{--O})_2\text{B}\text{--OH}$ and $(\text{--O})_2\text{P}(\text{O})\text{OH}$ groups and may be useful for further assignments as there is still uncertainty about the shift ranges for such groups. The shifts of 3.2 and 0.7 ppm (models 19 and 20) predicted for terminal POH and AlOH groups, respectively, on AlPO surfaces compare with shifts of 2.9 and -0.5 ppm, respectively, measured for aluminum phosphate catalysts.³³ They also fit into the ranges calculated and observed for POH and free $^{\text{IV}}\text{Al}\text{--OH}$ groups in general (Table III).

The calculated shifts in the free protonated H_3O^+ and $\text{CH}_3\text{--OH}_2^+$ species relative to H_2O and CH_3OH , respectively, are 7.4 and 6.2 ppm (cf. Table I). The free cations cannot be observed, of course. From liquid-phase experiments a shift of 14.5 ppm was estimated for the proton in H_3O^+ relative to that in H_2O .³⁴ Previous theoretical studies yielded 9.0 ppm.³⁵ Proton shifts

(32) Engelhardt, G.; Jerschke, H.-G.; Lohse, U.; Sarv, P.; Samoson, A.; Lippmaa, E. *Zeolites* 1987, 7, 289.

(33) Mastikhin, V. M.; Zamaraev, K. I. *Z. Phys. Chem. (Frankfurt/Main)* 1987, 152, 59.

(34) Akitt, J. W. *J. Chem. Soc., Dalton Trans.* 1973, 49.

(35) Fukui, H.; Miura, K.; Yamazaki, H.; Nosaka, T. *J. Chem. Phys.* 1985, 82, 1410.

(30) Harmony, M. D.; Laurie, V. W.; Kuezkowski, R. L.; Schwendeman, R. H.; Ramsay, D. A.; Lovas, F. J.; Lafferty, W. J.; Maki, A. G. *J. Phys. Chem. Ref. Data* 1979, 8, 619.

(31) Hill, J. R.; Sauer, J.; Ahlrichs, R. *Mol. Phys.* 1991, 73, 335.

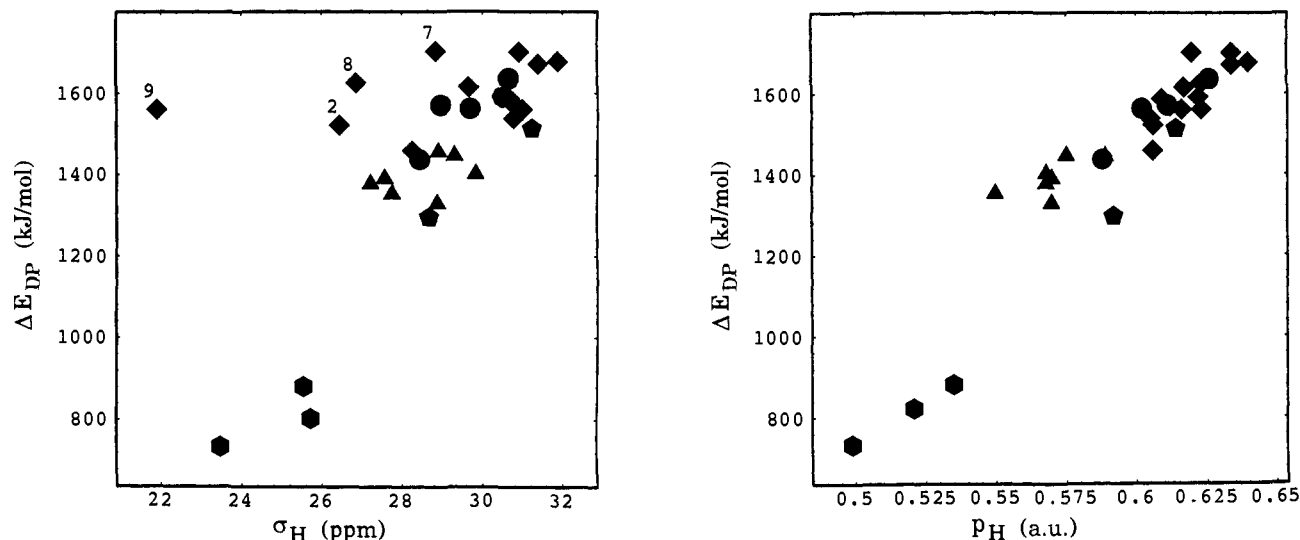


Figure 2. Plot of the dependence of the deprotonation energies, ΔE_{DP} , on (a, left) the shielding constants of the acidic proton, σ_H , and (b, right) the Mulliken electron population on the acidic hydrogen, p_H . The numbering refers to Table I. The symbols refer to the following subsets of related molecules: The \blacklozenge is used for the systematic series H_nXOH , with $X/n = H/0, B/2, C/3, N/2, O/1, F/0, Al/2, Si/3, P/2, S/1, Cl/0$, and for the substitution products C_2H_5OH , CF_3OH , and CF_3CH_2OH . The \bullet is used for $B(OH)_3$, $Al(OH)_3$, $Si(OH)_4$, and $OP(OH)_3$. The \bullet is used for the protonated species H_3O^+ , $CH_3OH_2^+$, and $P(OH)_4^+$ and \bullet for the H_3AlOPH_2OH and H_3POAlH_2OH models. The data for the $HO(H)Al(OH)_3$, $H_3SiO(H)Al(OH)_3$, $H_3SiO(H)AlH_3$, $H_3SiO(H)BH_3$, $(AlH_2OH)_2$, and $((HO)_2AlOH)_2$ models are represented by the \blacktriangle .

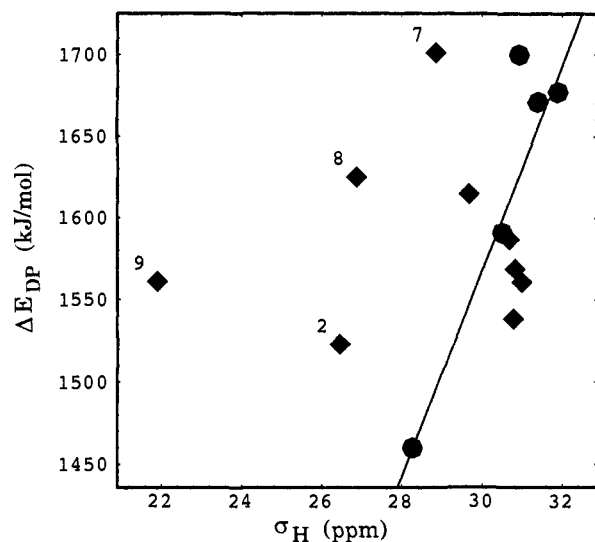


Figure 3. Same as Figure 2a, except data set is limited to H_nXOH molecules, with $X/n = H/0, B/2, N/2, O/1, F/0, Al/2, Si/3, P/2, S/1, Cl/0$ (\blacklozenge), and to the alcohols CH_3OH , C_2H_5OH , CF_3CH_2OH , and CF_3OH (\bullet). The regression line (slope 63 ± 4 kJ/(mol·ppm)) is for the four alcohols only (correlation coefficient $r = 0.99$).

between 5.3 and 9.1 ppm have been reported for $CH_3OH_2^+$ adsorbed on hydrogen forms of different zeolites.³⁶

Figure 2a correlates the calculated deprotonation energies with the calculated shielding constants. Three sets of data show a rough linear overall trend: (1) weakly acidic, all free XOH groups except CF_3OH , H_3PO_4 , and H_3AlOPH_2OH ; (2) acidic, all bridging groups plus CF_3OH , H_3PO_4 , and H_3AlOPH_2OH ; and (3) very acidic, all protonated species. It is the latter group of data with its very low deprotonation energies that saves the impression of a linear trend. This is quantified in Table IV, which shows correlation coefficients and standard deviations for various plots: When the cations are excluded, the correlation coefficients drop.

Within the individual data groups there is a wide scatter. Figure 3 shows the data of the H_nXOH molecules and all alcohols

separately. The points for CH_3OH , C_2H_5OH , CF_3CH_2OH , and CF_3OH form a straight line in accordance with the experimental work of Chauvel and True.⁹ BH_2OH , NH_2OH , H_2O_2 , and FOH show the largest deviations from an assumed linear trend. If they are excluded, the correlation r reaches 0.91, even if only neutral systems are considered (Table IV). Their second-row counterparts AlH_2OH , PH_2OH , $HSOH$, and $ClOH$ together with SiH_3OH cluster around the line, but show no correlation among each other.

The plot of the deprotonation energy against the Mulliken electron population (Figure 2b) shows a much better correlation ($r = 0.94$, cf. Table IV); there are no points with particularly large deviations. This is not true, however, for the plot of the shielding constants against the Mulliken electron population (Figure 4a, $r = 0.53$). No improvement could be reached when the calculation of electron populations was based on the orthogonalized minimal basis set approximation (OMBA).³⁷ This approximation was considered because it is expected to be less dependent on basis set details when a population analysis is performed for extended basis sets.

Within a picture of Boys-localized orbitals, the electron population on the H atom is dominated by the details of the OH bond orbital. Consequently and in accord with previous experience,²⁵ the OH bond orbital contribution to the shielding constant shows a better correlation with the electron population on H (Figure 4b, $r = 0.89$, cf. Table IV). This indicates that the contributions of the orbitals other than the OH bond orbital which are localized in the O atom of the OH group, namely the lone pairs and the XO bond orbital, are significant and not constant within the set of molecules studied. Within the first-row and second-row H_nXOH series (X from B to F and Al to Cl, respectively) the variation of the contribution of the OX bond (2.0 and 1.8 ppm, respectively, see Table I) is larger than that of the OH bond (1.2 and 0.2 ppm, respectively, see Table I). It is this variation of the non-OH-bond contributions that spoils a possible linear correlation between shielding constant and electron population on H and, hence, between shielding constant and deprotonation energy. Unfortunately, the OH bond orbital contribution to the chemical shift cannot be measured.

(37) Kollmar, H. *Theor. Chim. Acta* **1978**, *50*, 235.

(36) Anderson, M. W.; Barrie, P. J.; Klinowski, J. *J. Phys. Chem.* **1991**, *95*, 235.

(38) Mastikhin, V. M.; Mudrakovsky, I. L.; Shmachkova, V. P.; Kotsarenko, N. S. *Chem. Phys. Lett.* **1987**, *139*, 93.

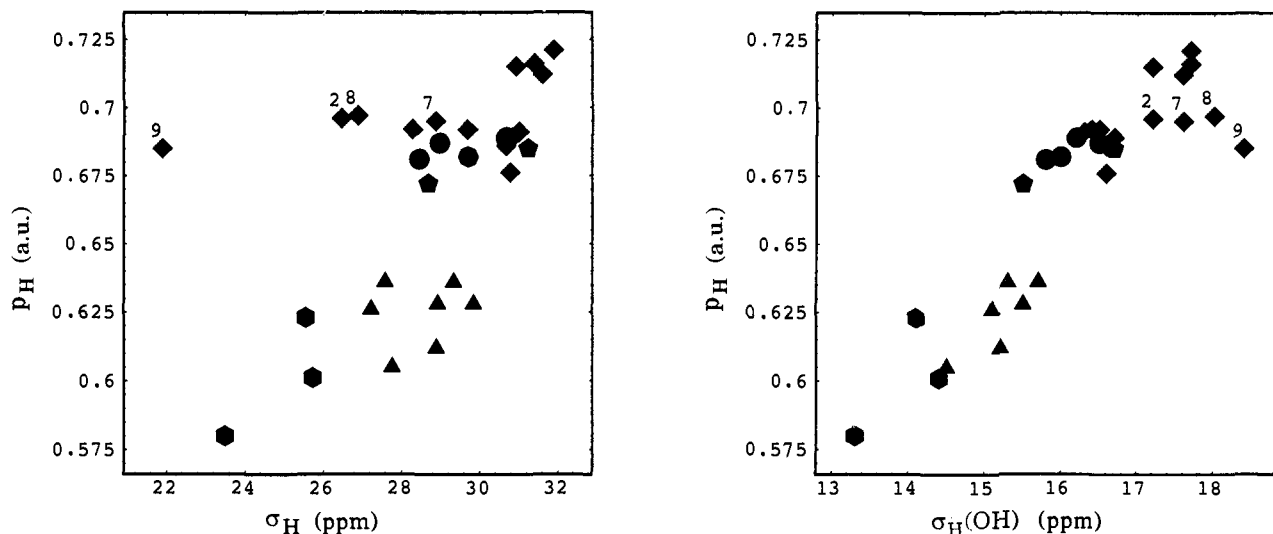


Figure 4. Plot of the Mulliken electron populations p_H against the shielding constants on the acidic hydrogen, σ_H . Different symbols refer to different subsets of related molecules (see Figure 2). The number refers to Table I. (a, left) Electron populations against total shielding constants. (b, right) Electron populations against the *OH* bond contribution to the shielding constants.

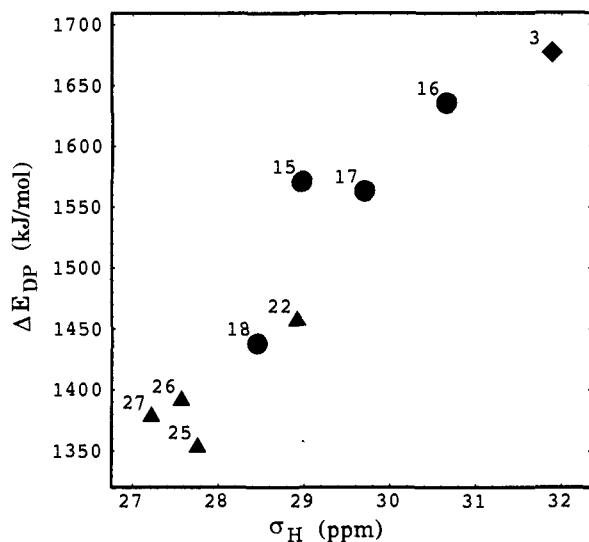


Figure 5. Same as Figure 2a, but the data set is limited to molecules that are relevant as models of surface hydroxyl groups. The methanol molecule has been included as a reference only.

From Figure 2 we reach the conclusion that, for most different molecules with XOH groups, ^1H NMR chemical shift data cannot be used to predict gas-phase acidities. The surface hydroxyl

groups which are responsible for the Brønsted acidity of catalysts, however are all bonded to atoms (B, Al, Si, or P) whose first coordination sphere consists of oxygen atoms only. The question is whether a correlation exists for this limited set of systems as it has been found by Chauvel and True for 9 alcohols within a range extending over 70 kJ/mol and 1.5 ppm.⁹ Figure 5 shows the data for those of our models that have the property of a complete oxygen coordination around the B, Al, Si, or P atoms (the methanol molecule has been included as a reference only). It appears that these points, which extend over a wider range of 300 kJ/mol and 4 ppm, are reasonably close to a straight line to render an acidity prediction based on proton chemical shifts meaningful. The slope of the regression line (methanol excluded) is 84 ± 12 kJ/(mol·ppm), and the correlation coefficient is $r = 0.93$. For the alcohols, Chauvel and True⁹ report a slope of 43 ± 2 kJ/(mol·ppm) with $r = 0.99$. The dependence of the slope on the subset considered reflects the fact that a linear relation does not exist for compounds containing hydroxyl groups in general.

Acknowledgment. The IGLO calculations have been performed on the CYBER 205 of the Rechenzentrum der Ruhr-Universität Bochum. Support from the 'Fonds der Chemischen Industrie' is greatly acknowledged. J.S. would like to thank Professor H. Pfeifer, University of Leipzig, and his co-workers for many valuable discussions.